Real-space renormalisation group study of selective site percolation on triangular lattice

1983 J. Phys. A: Math. Gen. 16 2501

(http://iopscience.iop.org/0305-4470/16/11/020)

J. Phys. A: Math. Gen. **16** (1983) 2501–2514. Printed in Great Britain

Real-space renormalisation group study of selective site percolation on triangular lattice

Toshihiro Idogaki and Norikiyo Uryû

Department of Applied Science, Faculty of Engineering, Kyushu University, Fukuoka 812, Japan

Received 22 November 1982, in final form 7 February 1983

Abstract. The selective site percolation is studied on three kinds of triangular lattice, TC, TK and TH lattices, by using renormalisation groups. The recursion relations on occupation probabilities are solved to give global phase diagrams with scaling factor $b = \sqrt{3}$, 2 and 3 for the TC lattice, and with $b = \sqrt{3}$ and $\sqrt{7}$ for TK and TH lattices respectively. The phase boundaries are obtained correctly with the flow direction towards a single isotropic fixed point. This result is in accordance with the anisotropic bond result and consistent with the universality hypothesis. In the extreme anisotropy limit of site preference, these boundaries give good estimates of the critical concentration p_c of chain, Kagomé and honeycomb lattices. Especially, in the chain limit for the TC lattice, the critical exponents of both the correlation length $\nu = 1$ and the dimensionality crossover $\phi = 1$ are reproduced exactly. The dependence of total p_c on site selectivity is also discussed.

1. Introduction

The percolation problem has been extensively studied because of its applicability to a variety of physical phenomena and its close relationship with thermal phase transitions (see e.g. Essam 1972, Stauffer 1979). The extension of the simple site and bond percolations to several directions has also been tried, for example correlated site, directed bond and combined site–bond percolation etc (Zhang 1982, Essam and De'Bell 1981, Guttmann and Whittington 1982, and references therein).

The anisotropic bond percolation is another example of such extensions. In this problem, different occupation probabilities are assumed for bonds placed in different coordinate directions. This model was first introduced for spatial dimensionality $d = 2$ (Sykes and Essam 1963) and later studied in detail for all d (Redner and Stanley 1979). The primary reason for studying this anisotropic model is to describe the dimensional crossover behaviour between different d. In recent years, the renormalisation group transformation (RGT) was applied to the problem for $d = 2$ by various authors (Ikeda 1979, Chaves *et al* 1979, de Magalhães *et al* 1981, Nakanishi *et al* 1981, Oliveira 1982), and the exact phase boundary with exact exponents for both crossover $\phi = 1$ and correlation length $\nu = 1$ in the chain limit was reproduced successfully (Oliveira 1982).

In contrast to the above, the corresponding inhomogeneous site percolation, or the percolation on a lattice having anisotropy of site preference, has been much less studied. Recently, Scholl and Binder (1980) have proposed the selective site percolation (SSP) in a two-sublattice system, assuming different occupation probabilities for

both sublattices. They paid particular attention to the case of spinel structure, and the critical exponent and the critical concentration p_c have been calculated by the Monte Carlo method. In a previous letter (Idogaki and Uryû 1982a), we considered the SSP on a square lattice by using RGT. With interactions up to the third neighbour, it was found that the SSP offers a simple method to estimate the p_c for homogeneous classical site percolation (CSP), and the applicability of the idea to other lattice structures was suggested.

In this paper, we study the SSP on a triangular lattice, in which two inequivalent sites A and B with independent occupation probabilities p_A and p_B are distributed regularly. We consider three kinds of distribution, triangular-chain (TC), triangular-Kagomé (TK) and triangular-honeycomb (TH) lattices as shown in figure 1. Interactions are assumed between all neighbouring sites. These systems show the crossover from the isotropic triangular lattice at $p_A = p_B$ to the chain, Kagomé and honeycomb lattices, respectively, in the extreme anisotropy limit of $p_B = 0$. Those systems have two distinct phases depending on the p_A and p_B values, the percolating phase and the non-percolating one. In the latter phase, all occupied sites fall into a number of finite clusters, while there appears an infinite network of occupied sites in the former phase.

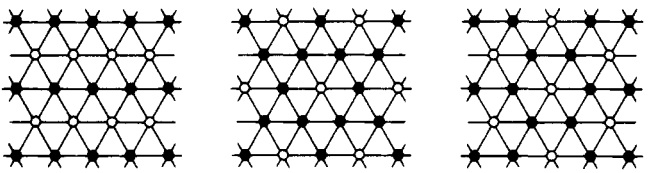

Figure 1. Various two-sublattice configurations on a triangular lattice: (*a*) triangular-chain (TC), (*b*) triangular-Kagomé (TK) and (*c*) triangular-honeycomb (TH) lattices. The full and open circles represent the A and B sites with occupation probabilities p_A and p_B, respectively.

The purpose of this paper is to give the global phase diagram for three lattices and to study the critical behaviour of SSP. In general, the standard percolation problem and its variants, for example correlated site and anisotropic bond etc, are believed to belong to the same universality class and thus have the same critical exponents (Zhang 1982, Guttmann and Whittington 1982, Oliveira 1982). However, it is claimed that this is not the case for directed percolation (Kertész and Vicsek 1980). Then, it is significant to check the question in the present case. The TC lattice gives a site version of the dimensional crossover between $d = 1$ and $d = 2$, which has been well investigated for the bond case as mentioned previously. In particular, it is firmly believed that the bond and site percolation problems reveal the same critical behaviour since they are interconnected through the concept of a covering lattice (Sykes and Essam 1964). So the aim of studying the TC lattice is twofold: a direct interest for the site problem and a verification of the bond results from a different point of view. The preliminary result for the TC lattice was reported by Idogaki and Uryû (1982b).

The simplest way to discuss the phase boundary of the problem is to approximate the regular distribution of TC, TK and TH lattices by the triangular-random (TR) lattice, in which A and B sites are distributed randomly with the same concentration c_A and c_B of A and B sites as those of the original regular lattices.

Owing to its perfect randomness, an arbitrary site on a TR lattice is occupied with the same averaged occupation probability: $p = c_A p_A + c_B p_B$. The critical concentration for the isotropic triangular lattice is known exactly and is given by $p_c = \frac{1}{2}$ (Sykes and Essam 1963). Then, the percolating region in the parameter space is directly given by

$$c_A p_A + (1 - c_A) p_B \geqslant \tfrac{1}{2}, \tag{1.1}$$

with the use of the relation $c_A + c_B = 1$. The phase diagram obtained by this random distribution approximation (RDA) is shown in figure 2. If we put $c_A = \frac{1}{2}$, $\frac{3}{4}$ and $\frac{2}{3}$, we get the following phase boundaries for each lattice:

$$\begin{aligned} &p_A^c + p_B^c = 1 && \text{TC lattice} \\ &3p_A^c + p_B^c = 2 && \text{TK lattice} \\ &4p_A^c + 2p_B^c = 3 && \text{TH lattice.} \end{aligned} \tag{1.2}$$

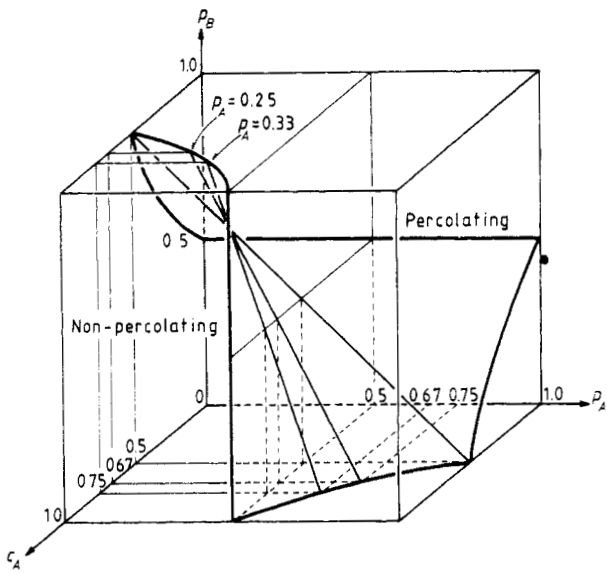

Figure 2. The percolation phase diagram for the TR lattice in the parameter space of p_A, p_B and c_A $(=1-c_B)$.

Equation (1.2) for the TC lattice coincides with the exact one obtained by Ikeda (1979) using graph theory. Now we define the anisotropy parameter $\gamma = p_B/p_A$, which represents the degree of site preference. For TK and TH lattices, the total critical concentration $p_c = c_A p_A^c + c_B p_B^c$ is expected to depend on γ, since the topological geometries of two sublattices are non-equivalent for these lattices. For all the lattices, however, we found that equation (1.2) gives a constant value of $p_c = \frac{1}{2}$ independent of γ. This shows that the critical line by the RDA is not accurate in the whole region of p_A and p_B except for the TC lattice. In any case, it is impossible to calculate the critical exponent and to discuss the universality class of SSP by this simple RDA.

In the present article, we study the SSP on the triangular lattice by applying the RGT developed in previous papers (Idogaki and Uryû 1982a, 1982b). A preferred-cell to preferred-site transformation keeping the original lattice symmetry is expected to

give correct phase diagrams in the whole region. The extension of the parameter space enables us to get new estimates of p_c for Kagomé and honeycomb lattices which can be used to check the accuracy of the present calculation. Furthermore, from the flow direction on the phase boundary, it will be possible to check the universality hypothesis. In § 2, we first summarise the two-parameter RGT. Then, the theory is applied to TC, TK and TH lattices by using the three-site cell scaling. In § 3, a similar calculation is performed by using the large-cell division to confirm the result in § 2. Finally in § 4, a summary of the results is given with some concluding remarks.

2. Renormalisation group transformation

2.1. Basic theory

In this section, we give a brief description of the RGT (see e.g. Niemeyer and Van Leeuwen 1976, Ma 1976) applied to the two-parameter percolation problem (Reynolds *et al* 1977a). The RGT starts from partitioning a d-dimensional lattice into cells of b^d sites. Each cell has the role of a renormalised site preserving its original lattice symmetry. The original and the renormalised occupation probabilities are related by a certain prescription as (see §§ 2.2 and 3):

$$p'_\alpha = R_\alpha(\{p_\alpha\}) \qquad \alpha = A, B. \tag{2.1}$$

Those recursion relations have a 'fixed point' $\{p^*_\alpha\}$ satisfying

$$p^*_\alpha = R_\alpha(\{p^*_\alpha\}) \qquad \alpha = A, B. \tag{2.2}$$

Since the RGT decreases the lattice spacing by a scaling factor b, the mean size of a connected cluster ξ is expected to obey the relation

$$\xi(\{p'_\alpha\}) = b^{-1}\xi(\{p_\alpha\}) \qquad \alpha = A, B. \tag{2.3}$$

Equation (2.3) shows that the fixed point physically corresponds to either $\xi = 0$ or $\xi = \infty$, and thus the percolation threshold at which $\xi = \infty$ is to be associated with a non-trivial fixed point of equation (2.2).

For the discussion of the critical exponent, we expand p'_α around the non-trivial fixed point as

$$\delta p'_\alpha = \sum_\beta T^*_{\alpha,\beta}\delta p_\beta + \ldots \qquad \alpha, \beta = A, B \tag{2.4}$$

where $\delta p_\alpha = p_\alpha - p^*_\alpha$ and $T^*_{\alpha,\beta}$ means $\partial p'_\alpha/\partial p_\beta$ evaluated at the fixed point. The linearised RGT matrix $[T^*_{\alpha,\beta}]$ gives eigenvalues λ_i $(\lambda_1 \geqslant \lambda_2)$ and the corresponding left and right eigenvectors are (ψ^i_A, ψ^i_B) and (x^i_A, x^i_B), respectively. The normal coordinates introduced by

$$\delta u_i = \sum_\alpha \psi^i_\alpha \delta p_\alpha \qquad \alpha = A, B \tag{2.5}$$

transform as $\delta u'_i = \lambda_i \delta u_i$ under the scaling. The subspace $\{\delta u_i = 0\}$ for $\lambda_i > 1$ defines the critical surface, on which all points are driven to the fixed point by successive RGT.

From equations (2.2)–(2.5), ξ satisfies the relation

$$\xi(p) = b\xi\left(p^* + \sum_i \lambda_i \delta u_i e_i + \ldots\right) \tag{2.6}$$

where

$$p = \sum_{\alpha} p_\alpha e_\alpha \qquad e_i = \sum_{\alpha} x_\alpha^i e_\alpha \qquad \alpha = A, B \text{ and } i = 1, 2 \tag{2.7}$$

and e_α is the unit vector along the p_α axis. With the use of the scaling power y_i defined by $\lambda_i = b^{y_i}$ and setting $b = (\delta u_1)^{-1/y_1}$, equation (2.6) can be written as

$$\xi(p) = (\delta u_1)^{-1/y_1} \xi(p^* + e_1 + \delta u_2 (\delta u_1)^{-\phi} e_2 + \ldots) \tag{2.8}$$

with the crossover exponent $\phi = y_2/y_1$. If $\lambda_1 > 1 > \lambda_2$ and $\delta u_2 (\delta u_1)^{-\phi} \simeq 0$, the critical behaviour of ξ is represented by

$$\xi \propto (\delta u_1)^{-1/y_1} = (\delta u_1)^{-\nu} \tag{2.9}$$

where

$$\nu = y_1^{-1} = \ln b / \ln \lambda_1 \tag{2.10}$$

describes the divergence of the mean size of finite clusters, i.e. ν is the analogue of the thermal correlation length exponent.

2.2. Recursion relation and fixed point

The RGT mentioned above is applied to the TC, TK and TH lattices. We consider the simplest three-site scaling of $b = \sqrt{3}$. The basic scaling procedure is shown in figure 3. For the convenience of calculation, we distinguish the two types of cell which appear in figure 3. The first is the type-I cell which includes only one kind of site A or B, and the second is the type-II cell which includes both A and B sites. In the scaling, we transform the cell having the larger number of α-sites ($\alpha = A$ or B) into a new α-site with renormalised occupation probability p'_α. Following Reynolds *et al* (1977a), we count p' by a majority rule, i.e. a cell is defined as occupied if and only if all three sites or any two sites are occupied. This rule gives the probabilities for getting across the cell as

$$\begin{aligned} R_M^{\mathrm{I}}(p_\alpha) &= p_\alpha^3 + 3p_\alpha^2(1-p_\alpha) \\ R_M^{\mathrm{II}}(p_\alpha, p_\beta) &= p_\alpha^2 p_\beta + p_\alpha^2(1-p_\beta) + 2p_\alpha(1-p_\alpha)p_\beta \end{aligned} \tag{2.11}$$

for type-I and type-II cells, respectively.

As seen from figure 3, the TC lattice can be scaled by two kinds of type-II cell which are mutually translated by $p_A \leftrightarrow p_B$ permutation. The recursion relations are given by

$$p'_A = R_M^{\mathrm{II}}(p_A, p_B) \qquad p'_B = R_M^{\mathrm{II}}(p_B, p_A). \tag{2.12}$$

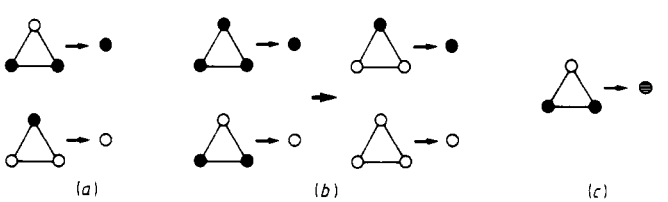

Figure 3. The renormalisation transformation by $b = \sqrt{3}$ scaling for (*a*) TC, (*b*) TK and (*c*) TH lattices. The full and open circles show the original (or renormalised) A and B sites, respectively. The hatched circle represents the unicolour site after renormalisation for the TH lattice.

For the TK lattice, both type-I and type-II cells appear. In this case, the geometrical array of renormalised A and B sites is perfectly inverted from the original one under the scaling. Then, the following successive twofold scaling is required to reproduce the original lattice symmetry:

$$p'_A = R^{\mathrm{II}}_M(R^{\mathrm{II}}_M(p_A, p_B), R^{\mathrm{I}}_M(p_A)) \qquad p'_B = R^{\mathrm{I}}_M(R^{\mathrm{II}}_M(p_A, p_B)). \tag{2.13}$$

From equations (2.12) and (2.13), it is obvious that if $p_\alpha \geqslant p_\beta$, the relation $p'_\alpha \geqslant p'_\beta$ always holds ($\alpha, \beta = A, B$). Contrary to the above, for the TH lattice, type-II cells of only one kind appear and the renormalised sites become colourless, i.e.

$$p'_A = p'_B = R^{\mathrm{II}}_M(p_A, p_B). \tag{2.14}$$

It is easily seen that equations (2.12)–(2.14) have two trivial fixed points $(p^*_A, p^*_B) = (0, 0)$ and $(1, 1)$ at which $\xi = 0$. For all lattices, we found a non-trivial fixed point $(p^*_A, p^*_B) = (\frac{1}{2}, \frac{1}{2})$ corresponding to the isotropic triangular lattice, with additional ones $(1, 0)$ and $(0, 1)$ in the chain limits for the TC lattice. From equation (2.10), the correlation length exponents $\nu(d)$ at the fixed points of isotropic and chain limits are calculated as $\nu(2) = 1.355$ and $\nu(1) = 0.792$, respectively. The expected values are $\nu(2) = \frac{4}{3}$ (den Nijs 1979, Derrida and de Seze 1982) and $\nu(1) = 1$ (Reynolds *et al* 1977b). Near the isotropic fixed point, the phase boundary is well represented by the linear approximation of equation (2.5) by setting $\delta u_1 = 0$, and the results agree with those given in equation (1.2).

2.3. Phase diagram

To obtain the precise phase boundary in the whole region, we should not restrict ourselves to the linear approximation. By starting from some initial points, we iterate the recursion relations on the computer. The flow trajectory enables us to obtain the entire phase diagram. The results for TC and TK lattices are shown in figures 4 and 5, respectively. The whole parameter space is divided into two regions depending upon whether the points converge to the fixed point $(0, 0)$ or converge to $(1, 1)$. As a result, we get a critical line which separates the percolating and non-percolating regions. On the critical line, the iteration flows towards the isotropic fixed point. This means that the critical behaviour of SSP is similar to that of CSP on the same lattice. On the other hand, the chain limits of the TC lattice are perfectly unstable and belong to the different universality class of $d = 1$. These results are consistent with the results obtained in the anisotropic bond percolation on the square lattice by Oliveira (1982). The full RGT calculation is impossible for the TH lattice, since it becomes colourless. So we have approximated the critical line by replacing p'_α in equation (2.14) with $\frac{1}{2}$: the critical concentration of the resulting unicolour system. The result is also shown in figure 5. This partial scaling has already come up earlier in the context of the three-colour site problem by Kondor (1980).

The critical line for the TC lattice is given by $p^{\mathrm{c}}_A + p^{\mathrm{c}}_B = 1$ and coincides with the exact one by Ikeda (1979). The critical lines for TK and TH lattices are not straight and at $p_B = 0$ they give $p^{\mathrm{c}}_A = 0.6534$ and $p^{\mathrm{c}}_A = 0.7071$, respectively. These values are in fair agreement with the values 0.6527 and 0.6962 known for the Kagomé (Sykes and Essam 1963) and honeycomb lattices (Djordjevic *et al* 1982), respectively. In the extreme case of $p_B = 1$, TK and TH lattices represent the Kagomé and honeycomb lattices, including up to third neighbour interactions; Kagomé* and honeycomb*,

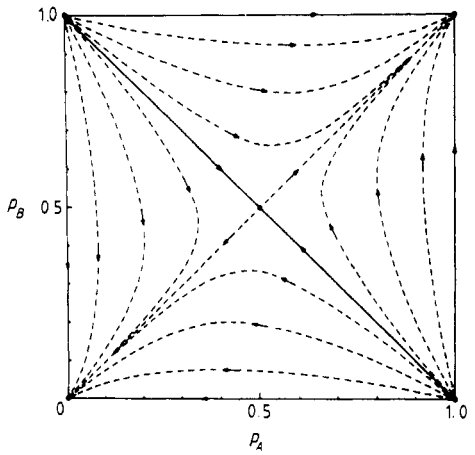

Figure 4. Flow diagram for the TC lattice obtained by $b=\sqrt{3}$ scaling. The full line is the critical line which separates the percolating and non-percolating regions. The arrows indicate the direction of flow. The full circles show the fixed points.

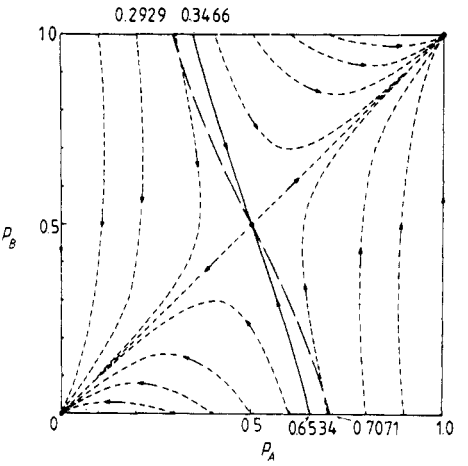

Figure 5. As figure 4 for the TK lattice. For comparison, the phase boundary for the TH lattice due to partial scaling is shown by the chain curve.

respectively. According to Sykes and Essam (1964), Kagomé* (honeycomb*) is the matching lattice of Kagomé (honeycomb) satisfying

$$p_c(L)+p_c(L^*)=1 \tag{2.15}$$

where $p_c(L)$ denotes the p_c for the L lattice. This matching condition between the systems of $p_B=0$ and $p_B=1$ is correctly reproduced in figure 5 for both TK and TH lattices.

From figures 4 and 5, we can calculate the dependence of the total critical concentration $p_c=p_A^c+p_B^c$ on site selectivity γ defined by $\gamma=p_B/p_A$. The results are shown in figure 6. Except for the TC lattice, the total p_c obviously depends on γ, and the dependence is strongly enhanced for the TH lattice. For $\gamma<1$, p_c decreases from the value $p_c=\frac{1}{2}$ of the isotropic case with a decrease of γ, while for $\gamma>1$, p_c increases from $\frac{1}{2}$ with an increase of γ up to some finite value p_c^0 characteristic of each lattice. The present calculation gives $p_c^0=0.510$ and 0.529 for TK and TH lattices, respectively. The global γ dependence of p_c can be explained reasonably by the variation of occupation for the A sublattice which plays an essential role in the build up of the infinite network. The presence of the upper limit p_c^0 is due to the fact that at $p>c_A\gamma^{-1}+c_B$ all additional particles are compulsively located on the A sublattice regardless of the value γ since the B sites are already fully occupied. A similar saturation effect has been found for the SSP on the square lattice (Idogaki and Uryû 1982a).

3. Large-cell calculation

In § 2, we discussed the simplest $b=\sqrt{3}$ scaling. However, the scaling has the disadvantage of giving an unsatisfactory result of $\nu(1)$ for the TC lattice. Furthermore,

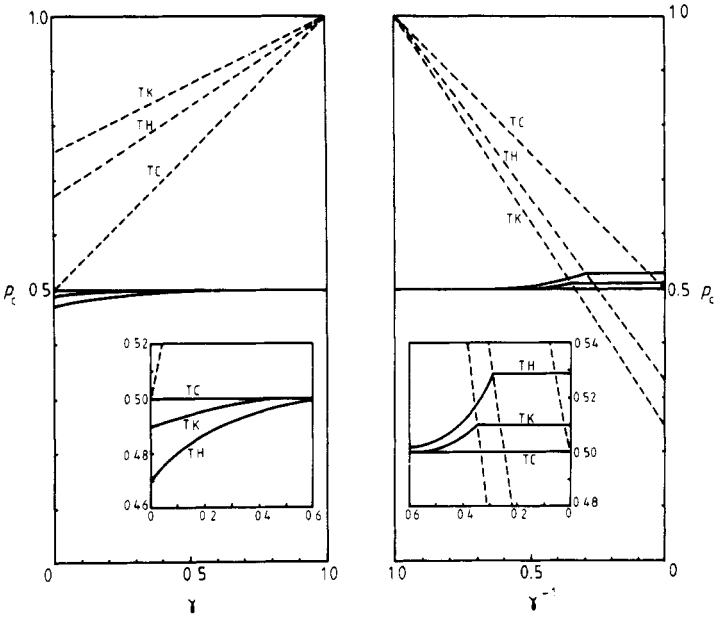

Figure 6. The variation of the total critical concentration p_c with the change of anisotropy parameter $\gamma = p_B/p_A$. The insets show magnifications of the strong anisotropy regions. The broken lines for $0 \leq \gamma \leq 1$ represent the concentrations above which all A sites are completely occupied, that is $p = (1+\gamma)/2$, $(3+\gamma)/4$ and $(2+\gamma)/3$ for TC, TK and TH lattices, respectively. Similarly, the broken lines for $1 \leq \gamma \leq \infty$ show the concentrations above which all B sites are fully occupied, i.e. $p = (\gamma^{-1}+1)/2$, $(3\gamma^{-1}+1)/4$ and $(2\gamma^{-1}+1)/3$ for those three lattices, respectively.

we have encountered a colourless problem for the TH lattice and we could not verify the universality relation for that case. In this section, we consider the larger-cell approximation to improve these points.

3.1. Square-like cell

A natural way to extend the cell size is to consider a square-like cell consisting of $b \times b$ sites (Idogaki and Uryû 1982b). This cell division was first done by Yuge (1978) for the isotropic triangular lattice, where he succeeded in getting an exact p_c and a good estimate of $\nu(2)$. For the square-like cell, three kinds of prescription have been proposed to obtain a renormalised occupation probability (Reynolds *et al* 1978). Namely, a cell is defined as occupied if a percolating path is spanning the cell, either horizontally or vertically (R_0 rule), or spanning in a single fixed direction (R_1) or spanning both ways (R_2). Reynolds *et al* (1980) have shown that all three transformations behave qualitatively the same way and only two of them are independent since $2R_1 = R_0 + R_2$. In the present study we use the R_1 rule, which gives the most rapid convergence of p_c (Reynolds *et al* 1980).

The $b = 2$ and $b = 3$ scalings for the TC lattice are shown in figure 7. In the scaling, the cell in which the α-site locates on a shorter diagonal line is transformed into a new α-site with p'_α. The transformation clearly assures the relation $p'_\alpha \geq p'_\beta$ when $p_\alpha \geq p_\beta$ and *vice versa*. By using the R_1 rule with an exclusion–inclusion principle, the

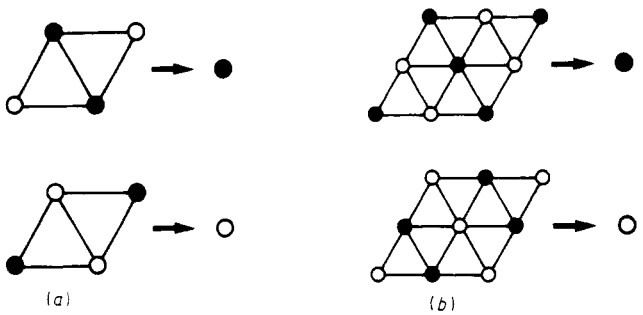

Figure 7. Transformation of the TC lattice by using a square-like cell of (*a*) $b=2$ and (*b*) $b=3$.

recursion relations for arbitrary b are given by

$$p'_A = R_1^{(b)}(p_A, p_B) \qquad p'_B = R_1^{(b)}(p_B, p_A) \tag{3.1}$$

where

$$R_1^{(b)}(p_A, p_B) = A_n + \sum_{i=1}^{n-1} A_i f_i(\{B_j\}). \tag{3.2}$$

In equation (3.2), n is the number of A sites in the cell, i.e. $n = b^2/2$ for even b and $(b^2+1)/2$ for odd b, and

$$A_k = p_A^k (1-p_A)^{n-k} \qquad B_l = p_B^l (1-p_B)^{b^2-n-l} \tag{3.3}$$

and $f_i(\{B_j\}) = f_i(p_B)$ are finite polynomials in p_B. For instance, the explicit formula of equation (3.2) is given by

$$\begin{aligned} R_1^{(2)}(p_A, p_B) &= A_2 + A_1(2B_2 + 2B_1) \\ R_1^{(3)}(p_A, p_B) &= A_5 + A_4(5B_4 + 20B_3 + 27B_2 + 14B_1 + 2B_0) \\ &\quad + A_3(10B_4 + 36B_3 + 40B_2 + 14B_1 + B_0) \\ &\quad + A_2(9B_4 + 26B_3 + 20B_2 + 4B_1) + A_1(3B_4 + 6B_3 + 3B_2) \end{aligned} \tag{3.4}$$

for $b=2$ and $b=3$, respectively, and so on.

As for $f_i(p_B)$, we can show $f_{n-1}(0) = n-b$ and $f_1(1) = b$ for arbitrary b (Idogaki and Uryû 1982b). Then, it is easily seen that equations (3.1) and (3.2) admit the following fixed points for any values of b; $(p_A^*, p_B^*) = (0,0)$, $(1,1)$, $(1,0)$ and $(0,1)$. Furthermore, if we note the matching relation for $R_1^{(b)}(p_A, p_B)$

$$R_1^{(b)}(p_A, p_B) + R_1^{(b)}(1-p_A, 1-p_B) = 1 \tag{3.5}$$

we find the additional isotropic fixed point at $(\frac{1}{2}, \frac{1}{2})$, and also find the exact phase boundary $p_A^c + p_B^c = 1$ for any b. The whole flow diagram has been calculated based on $b=2$ and $b=3$ scaling. The results agree perfectly with those of figure 4, except for a slightly fast convergence in successive iteration for $b=3$.

At each fixed point, the scaling powers $y_i(d)$ can be calculated from equation (2.10). In the chain limits $(1,0)$ and $(0,1)$, we find $T_{AA}^* = T_{BB}^* = b$ and $T_{AB}^* = T_{BA}^* = 0$. Then we get

$$y_i(d) = \ln \lambda_i / \ln b = \ln b / \ln b = 1 \qquad i = 1, 2 \tag{3.6}$$

which leads to

$$\nu(1) = y_1^{-1}(1) = y_2^{-1}(1) = 1 \qquad \phi = y_2(1)/y_1(1) = 1 \tag{3.7}$$

for any value of b. In the same way, at the isotropic fixed point $(\frac{1}{2}, \frac{1}{2})$, the exponent $\nu(2)$ is calculated as

$$\nu(2) = y_1^{-1}(2) = \begin{cases} 1.710 & b = 2 \\ 1.651 & b = 3 \end{cases} \tag{3.8}$$

and the conjectured value $\frac{4}{3}$ (den Nijs 1979) is expected to be approached with the increase of b. The results are tabulated in table 1. In the table, the result for the anisotropic bond percolation on a square lattice (Oliveira 1982) is shown for comparison. It should be noted that the present RGT calculation gives an exact $\nu(1)$ for any scaling of $b \geqslant 2$, in contrast with the bond approach.

Table 1. The RGT results of the correlation-length critical exponents $\nu(1)$ and $\nu(2)$ in site percolation, compared with those in bond percolation (Oliveira 1982). For both problems, the crossover exponent $\phi = 1$ is obtained exactly for any value of b.

	Bond		Site	
b	$\nu(1)$	$\nu(2)$	$\nu(1)$	$\nu(2)$
$\sqrt{3}$	—	—	0.792	1.355
2	0.631	1.042	1	1.710
3	0.683	1.099	1	1.651
4	0.712	—	1	1.624[a]
Expected[b]	1	$\frac{4}{3}$	1	$\frac{4}{3}$

[a] Yuge (1978).
[b] Reynolds *et al* (1977b), den Nijs (1979).

A similar calculation has been applied to the other lattices. For TK and TH lattices, however, we found that the direct application brings unicolour or three-colour problems for $b = 2$ and 3, and failed to complete the RGT calculation. This shows that the hexagonal character of TK and TH lattices cannot be reflected well by a square-like cell division, so the scaling by another type of cell is required for these lattices.

3.2. Hexagonal cell

For TK and TH lattices, we divide the lattice into a hexagonal cell with seven sites ($b = \sqrt{7}$). As a result of this, we have three types of the cell having different compositions of A and B sites, as shown in figure 8. In the transformation, the definition of occupation for a hexagonal cell is somewhat arbitrary and seems not to be established yet (Tatsumi 1980, Chakrabarti *et al* 1981). For the isotropic case, Tatsumi (1980) has used the arithmetic mean of the percolation probabilities between the sides bc and de, and between the sides abc and def. However, it cannot be directly applied to the type-II or type-III cells, since those cells have directional asymmetry of percolating paths.

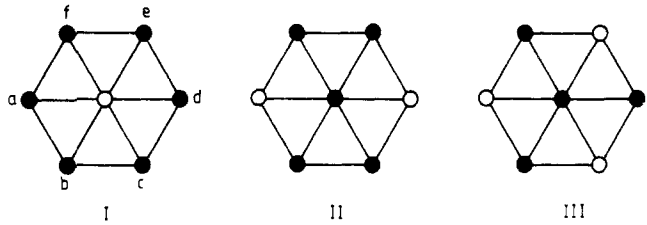

Figure 8. The three types of hexagonal cells which appear in the $b=\sqrt{7}$ scaling for TK and TH lattices.

Instead, we consider here an extension of rules R_0, R_1 and R_2 primarily adapted for the square-like cell. The spirit of these rules may be regarded as that R_0 requires the presence of a percolating path, at least, between one set of opposite planes, e.g. ab and de, and R_2 requires, at least, between two sets of them, i.e. a crossing of percolating flow within the cell. Consequently, for the hexagonal cell, we may define R_1 as the arithmetic mean of those R_0 and R_2 by analogy with the relation $2R_1 = R_0 + R_2$ for the square-like cell. In the following, we use this definition of R_1. The occupation probability for each type of cell can be calculated as follows:

$$\begin{aligned}
R_1^{\mathrm{I}}(p_A, p_B) &= A_6 + 6A_5 + 3A_4(5B_1 + 3B_0) + A_3(17B_1 + 3B_0) + 6A_2B_1 \\
R_1^{\mathrm{II}}(p_A, p_B) &= A_5 + A_4(5B_2 + 10B_1 + 4B_0) + A_3(10B_2 + 15B_1 + 3B_0) \\
&\quad + A_2(7B_2 + 5B_1) + A_1B_2 \qquad (3.9) \\
R_1^{\mathrm{III}}(p_A, p_B) &= A_4 + A_3(4B_3 + 12B_2 + 9B_1 + 1.5B_0) + A_2(6B_3 + 13.5B_2 + 4.5B_1) \\
&\quad + A_1(2.5B_3 + 3B_2)
\end{aligned}$$

where A_k and B_l are given by equation (3.3) but with $n = 6$, 5 and 4 for type-I, -II and -III cells, respectively.

For the TK lattice, type-I and -II cells appear. After successive twofold scaling as in § 3.2, the recursion relations are given by

$$p'_A = R_1^{\mathrm{II}}(R_1^{\mathrm{II}}(p_A, p_B), R_1^{\mathrm{I}}(p_A, p_B)) \qquad p'_B = R_1^{\mathrm{I}}(R_1^{\mathrm{II}}(p_A, p_B), R_1^{\mathrm{I}}(p_A, p_B)). \qquad (3.10)$$

For the TH lattice, type-I and -III cells appear and successive twofold scaling is also needed. The recursion relations are:

$$p'_A = R_1^{\mathrm{III}}(R_1^{\mathrm{III}}(p_A, p_B), R_1^{\mathrm{I}}(p_A, p_B)) \qquad p'_B = R_1^{\mathrm{I}}(R_1^{\mathrm{III}}(p_A, p_B), R_1^{\mathrm{I}}(p_A, p_B)). \qquad (3.11)$$

From equations (3.10) and (3.11), we found three fixed points $(p_A^*, p_B^*) = (0, 0)$, $(1, 1)$ and $(\frac{1}{2}, \frac{1}{2})$ for both lattices. At the fixed point $(\frac{1}{2}, \frac{1}{2})$, we get $\nu(2) = 1.508$ which is better than $\nu(2) = 1.767$ estimated by Tatsumi (1980) from a similar hexagonal-cell calculation on an isotropic triangular lattice. The whole flow diagram obtained by iteration calculation of equation (3.11) is shown in figure 9. As expected, the isotropic fixed point is stable for the anisotropy perturbation. This is consistent with the results in § 2 and also with the universality hypothesis. The flow diagram for the TK lattice is almost similar to that of figure 5 and is omitted here. The critical line intersects with the p_A axis at $p_A^c = 0.6573$ and $p_A^c = 0.7147$ for TK and TH lattices, respectively.

The extension of the calculation to a larger hexagonal cell of $b = \sqrt{19}$ is possible by using a computer but not performed here.

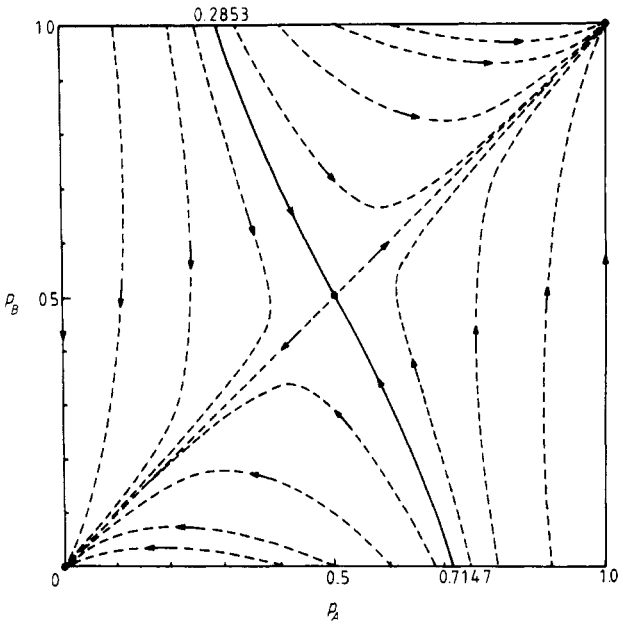

Figure 9. Flow diagram for the TH lattice by $b = \sqrt{7}$ scaling.

4. Summary and concluding remarks

We have studied the SSP on the TC, TK and TH lattices by RGT. First we performed the simplest $b = \sqrt{3}$ scaling and succeeded in obtaining precise phase diagrams for this two-parameter percolation problem. The critical lines gave good estimates of p_c for CSP in the extreme anisotropy limits and enabled us to obtain the dependence of total p_c on site selectivity. As regards the phase boundary, the RDA discussed in § 1 is equivalent to the linear approximation in RGT and is valid only for the region of $p_A \simeq p_B$ except for the TC lattice. From the analysis of critical flow direction, we have concluded that the anisotropy of site preference is an irrelevant parameter always leading to the same universality. Furthermore, the dimensional crossover between $d = 2$ and $d = 1$ has been obtained exactly for the TC lattice.

The calculation has been extended to larger b with a square-like cell consisting of 2×2 or 3×3 sites for the TC lattice and with a hexagonal cell of seven sites for TK and TH lattices. In the former the correlation length critical exponent $\nu(1) = 1$ has been obtained exactly in the chain limit. Also the larger-cell calculation enabled us to avoid the colourless problem for the TH lattice, and we could verify that the flow direction was consistent with the other two lattices.

The numerical results of p_c for CSP obtained from the critical line for SSP are summarised in table 2. The accuracy of the critical line does not seem to be improved by $b = \sqrt{7}$ scaling. This may be considered to be due to the inadequacy of the definition of p' adopted for the hexagonal cell. As shown by Reynolds *et al* (1980), however, the definition of p' itself plays a progressively smaller role with $b \to \infty$. Then we would expect the present approximation to become better as the cell size increases further.

Table 2. Critical concentration p_c for CSP, evaluated by SSP on the triangular lattice.

	RDA	RGT $b=\sqrt{3}$	RGT $b=\sqrt{7}$	Expected†
Chain	1	1	1	1
Triangular	$\frac{1}{2}$	$\frac{1}{2}$	$\frac{1}{2}$	$\frac{1}{2}$
Kagomé	$\frac{2}{3}$	0.6534	0.6573	0.6527
Honeycomb	$\frac{3}{4}$	0.7071	0.7147	0.6962

† Sykes and Essam (1963), Djordjevic *et al* (1982).

In principle, the present calculation can be directly extended to the three-dimensional case. We show some typical two-sublattice divisions of the SC lattice in figure 10. We consider the interactions up to nth neighbour and the scaling of $b=3$ by two sets of cells (IA, IB) and (II, III) shown in figures 10(a) and 10(b). For figure 10(a), we found that in the extreme limit of $p_\alpha = 0$ the SSP for $n=1$ gives the CSP on the FCC lattice for $n=2$. Also, it is found that SSP for $n=2$ gives the CSP on the FCC lattice for $n=1$ by putting $p_\alpha = 0$. For figure 10(b), in the same way, the SSP for $n=3$ gives the CSP on the BCC lattice for $n=1$ by putting $p_B = 0$. As in the case of $b=\sqrt{19}$ scaling for the TK and TH lattices, those three-dimensional calculations need comprehensive and elaborate numerical work to get p'_α. It will be an interesting future problem to perform the Monte Carlo renormalisation group calculation (Reynolds *et al* 1978, 1980) for those systems.

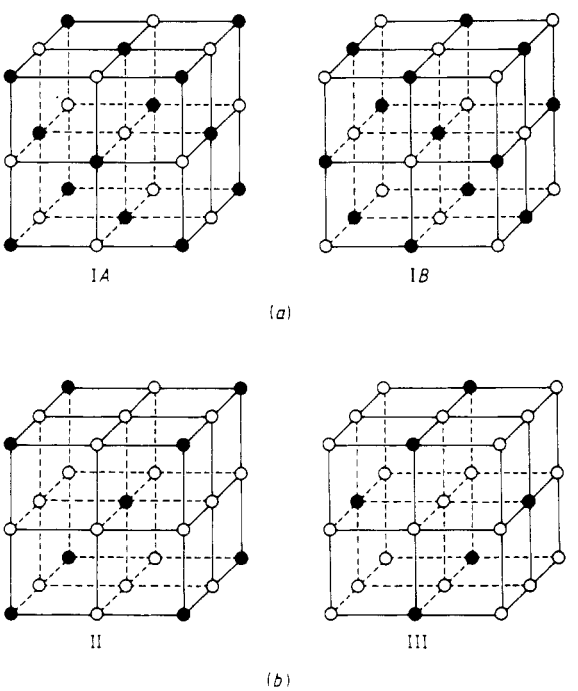

Figure 10. The typical two-sublattice divisions of the SC lattice, and the basic cells for $b=3$ scaling. For details, see the text.

References

Chakrabarti B K, Kaski K and Kertész J 1981 *Phys. Lett.* **82**A 97–9
Chaves C M, Oliveira P M, Riera R and de Queiroz S L A 1979 *Prog. Theor. Phys.* **62** 1550–5
Derrida B and de Seze L 1982 *J. Physique* **43** 475–83
Djordjevic Z V, Stanley H E and Margolina A 1982 *J. Phys. A: Math. Gen.* **15** L405–12
Essam J W 1972 *Phase Transitions and Critical Phenomena* vol 2, ed C Domb and M S Green (London: Academic) pp 197–270
Essam J W and De'Bell K 1981 *J. Phys. A: Math. Gen.* **14** L459–61
Guttmann A J and Whittington S G 1982 *J. Phys. A: Math. Gen.* **15** 2267–71
Idogaki T and Uryû N 1982a *Phys. Lett.* **90**A 367–9
—— 1982b *J. Phys. C: Solid State Phys.* **15** L1077–81
Ikeda H 1979 *Prog. Theor. Phys.* **61** 842–9
Kertész J and Vicsek T 1980 *J. Phys. C: Solid State Phys.* **13** L343–8
Kondor I 1980 *J. Phys. A: Math. Gen.* **13** L397–401
Ma S K 1976 *Modern Theory of Critical Phenomena* (New York: Benjamin)
de Magalhães A C N, Tsallis C and Schwahheim G 1981 *J. Phys. C: Solid State Phys.* **14** 1393–408
Nakanishi H, Reynolds P J and Redner S 1981 *J. Phys. A: Math. Gen.* **14** 855–71
Niemeyer Th and Van Leeuwen J M J 1976 *Phase Transitions and Critical Phenomena* vol 6, ed C Domb and M S Green (London: Academic) pp 425–505
den Nijs M P M 1979 *J. Phys. A: Math. Gen.* **12** 1857–68
Oliveira P M C 1982 *Phys. Rev.* B **25** 2034–5
Redner S and Stanley H E 1979 *J. Phys. A: Math. Gen.* **12** 1267–83
Reynolds P J, Klein W and Stanley H E 1977a *J. Phys. C: Solid State Phys.* **10** L167–72
Reynolds P J, Stanley H E and Klein W 1977b *J. Phys. A: Math. Gen.* **10** L203–9
—— 1978 *J. Phys. A: Math. Gen.* **11** L199–207
—— 1980 *Phys. Rev.* B **21** 1223–45
Scholl F and Binder K 1980 *Z. Phys.* **39** 239–47
Stauffer D 1979 *Phys. Rep.* **54** 1–74
Sykes M F and Essam J W 1963 *Phys. Rev. Lett.* **10** 3–4
—— 1964 *J. Math. Phys.* **5** 1117–27
Tatsumi T 1980 *Prog. Theor. Phys.* **64** 803–12
Yuge Y 1978 *Phys. Rev.* B **18** 1514–7
Zhang Z 1982 *Phys. Lett.* **91A** 246–8